



Computationally efficient buckling analysis of wind turbine towers

Sándor Ádány¹, Benjamin W. Schafer²

Abstract

In the research reported herein a computationally efficient numerical method is introduced for the buckling analysis of tubular structures. The method uses Fourier-series approximations for the displacement functions. The strain-displacement relationship directly considers the curved geometry of the tubular shell. The implementation allows for arbitrary support conditions. In the solution developed to date four pure loading situations, uniform along the member length, are considered: normal force, bending moment, torque, and shear force. However, these four basic cases can arbitrarily be combined, as is commonly occurring in wind turbine support towers. The applied methodology results in a computational advantage compared to shell FEM, fast enough to be utilized in preliminary or code-based designs, while still maintaining much more generality and applicability compared to common analytical solutions. In this paper the method is briefly presented, then illustrated by proof-of-concept examples.

1. Motivation

The supporting structures of wind turbines are tubular steel cantilevers. Since they are slender, buckling is important. Analytical buckling solutions are available in textbooks (see e.g., Donnell, 1933, Timoshenko and Gere, 1961, Flügge, 1962), but limited only for simple cases, i.e., members with simple supports subjected to simple loading such as pure compression or pure bending. Shell finite element calculation is available, too, but it requires a fine discretization (Mahmoud et al., 2017), and can lead to a large number of shell finite elements and degrees of freedom, especially if the analyzed member is long. Thus, shell FEM is computationally expensive, and can be demanding even with today's computers. Moreover, customizability of commercial FEM software is limited, hence it is usually impossible to control the underlying mechanical assumptions. These are some of the reasons there is still ongoing research effort to develop computationally efficient numerical methods for shells, see e.g., Sadovsky (2019).

A newly developed numerical stability analysis tool is introduced herein. The primary role of the method is the linear buckling analysis of tubular structures; however, it was supplemented with added features, such as spectral analysis, or buckling length calculation. These added features can

¹ Professor, Budapest University of Technology and Economics, <adany.sandor@emk.bme.hu>
Visiting Faculty Scholar, Johns Hopkins University, <asandor2@jhu.edu>

² Professor, Johns Hopkins University, <schafer@jhu.edu>

be employed not only on buckled shapes, but on any displacement field, including measured geometric imperfections of real tubes or displacements from a collapse analysis by FEM.

In this paper the focus is on linear buckling analysis. The method uses Fourier-series approximation for the displacement functions. The Fourier-series approximation does not require discretization; however, in our method longitudinal discretization can optionally be applied, i.e., the member can be divided into segments, and between the segments continuity criteria can be prescribed. Though this feature of the method is not discussed in this paper, it is beneficial, since it can enhance the numerical stability of the calculations, as well as it makes it possible to model non-uniform member geometry (i.e., tapering, a typical characteristics of wind turbine towers, see Ding et al., 2022) and/or non-uniform load distribution along the member length (again, typical for wind turbine towers).

In the following, first, the method is briefly introduced, then its application is illustrated by performing a large number of linear buckling analysis on simple uniform tubular members; however, these examples consider both pure and combined loads across a wide range of geometries. Further features of the developed method (e.g., tapered members, spectral analysis, etc.) will be presented in subsequent papers.

2. Brief summary of the method

2.1 The displacements

The studied tubular member is geometrically defined by its radius, R , thickness, t , and length, L , where the radius is interpreted as the mean of the radii of the outer and inner surfaces, see Fig. 1. For the description of the displacements we introduce a coordinate system. Three displacement functions are involved, u , v , and w , where v is longitudinal, i.e., in the y -direction, and u and w are transverse displacements: u being circumferential translation, and w being radial translation (in the x - and z -direction, respectively). Note, that x is a circumferential coordinate, i.e., the x -axis is curved.

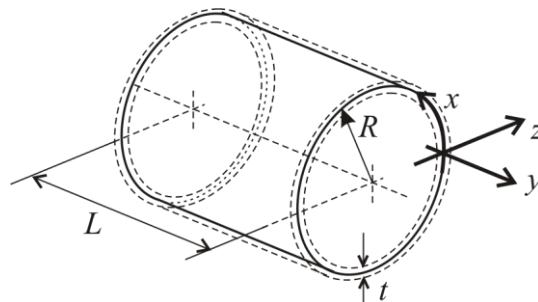


Figure 1: Coordinates, basic terminology

The displacement functions are approximated identically, by full Fourier series. Thus, any d displacement is approximated as:

$$d(x, y) = d_x(x) \cdot d_y(y) \quad (1)$$

with

$$d_x(x) = a_0 + \sum_{i=1}^p \left(a_{s,i} \sin \frac{2ix}{\pi} + a_{c,j} \cos \frac{2ix}{\pi} \right) \quad (2)$$

$$d_y(y) = b_0 + \sum_{j=1}^q \left(b_{s,j} \sin \frac{j\pi y}{L} + b_{c,j} \cos \frac{j\pi y}{L} \right) \quad (3)$$

Accordingly, the u , v , and w translations are expressed as:

$$u(x, y) = \sum_{k=1}^n u_k f_k(x, y) \quad v(x, y) = \sum_{k=1}^n v_k f_k(x, y) \quad w(x, y) = \sum_{k=1}^n w_k f_k(x, y) \quad (4)$$

where the $f(x,y)$ functions are trigonometric functions coming from the product of the x - and y -directional Fourier series, and n is the total number of Fourier terms, calculated from the number of terms in the circumferential and meridian directions (p and q , respectively):

$$n = (p + 1)(q + 1) \quad (5)$$

2.2 The strains

From the displacements the strains are calculated by directly considering the curved nature of the geometry. In particular, strains are similar to those in Silvestre (2007), (which are based on Sanders, 1963); however, with some modifications. To calculate the strains, first, the slopes (β) of the displacement functions are defined as the surface is rotated around the x -, y -, and z -axis:

$$\beta_x = -\frac{\partial w}{\partial y} \quad \beta_y = \frac{u}{R} - \frac{\partial w}{\partial x} \quad \beta_z = -\frac{\partial u}{\partial y} \quad (6)$$

From the slopes the curvatures (κ) are:

$$\kappa_{xx} = \frac{\partial \beta_y}{\partial x} \quad \kappa_{yy} = \frac{\partial \beta_x}{\partial y} \quad \kappa_{xy} = \frac{\partial \beta_x}{\partial x} + \frac{\partial \beta_y}{\partial y} + \frac{\beta_z}{R} \quad (7)$$

The linear strain components are as follows:

$$\varepsilon_x^L = \frac{\partial u}{\partial x} + \frac{w}{R} + z \kappa_{xx} \quad \varepsilon_y^L = \frac{\partial v}{\partial y} + z \kappa_{yy} \quad \gamma_{xy}^L = \frac{\partial v}{\partial x} + \frac{\partial u}{\partial y} + z \kappa_{xy} \quad (8)$$

The nonlinear components are as follows:

$$\varepsilon_x^{NL} = 0 \quad \varepsilon_y^{NL} = \frac{1}{2} (\beta_x^2 + \beta_z^2) \quad \gamma_{xy}^{NL} = \beta_x \beta_y \quad (9)$$

It can be observed that the second-order (nonlinear) hoop strains are disregarded, since these can be assumed to be fairly small for the considered loading cases; nevertheless, the nonlinear hoop strains can be added later.

2.3 Total potential

Isotropic, linear elastic material is considered. The internal part of the total potential is, therefore:

$$\Pi_{int} = \frac{1}{2} \int_0^L \int_0^{2R\pi} \int_{-t/2}^{+t/2} \boldsymbol{\varepsilon}_L^T \mathbf{D} \boldsymbol{\varepsilon}_L dx dy dz \quad (10)$$

where

$$\mathbf{D} = \begin{bmatrix} E & \nu E & 0 \\ \nu E & E & 0 \\ 0 & 0 & G \end{bmatrix} \quad (11)$$

$$\boldsymbol{\varepsilon}_L^T = [\varepsilon_x^L \quad \varepsilon_y^L \quad \gamma_{xy}^L] \quad (12)$$

and E and G are the Young's and shear modulus, respectively, and ν is the Poisson's ratio.

The external part of the total potential is calculated from the stresses and the nonlinear strains, as:

$$\Pi_{ext} = -t \int_0^L \int_0^{2R\pi} \boldsymbol{\varepsilon}_{NL}^T \boldsymbol{\sigma} dx dy \quad (13)$$

where

$$\boldsymbol{\varepsilon}_{NL}^T = [\varepsilon_x^{NL} \quad \varepsilon_y^{NL} \quad \gamma_{xy}^{NL}] \quad (14)$$

$$\boldsymbol{\sigma}^T = [\sigma_x \quad \sigma_y \quad \tau_{xy}] \quad (15)$$

The x -direction (hoop) normal stresses are disregarded, for the other two components uniform distribution is assumed in the longitudinal direction. In the circumferential direction the stress is assumed to be either constant or sinusoidal. Practically, 4 basic loading situations are considered:

- uniformly distributed σ_y stress creates pure compression (marked as 'N', or 'pure N');
- sinusoidally distributed σ_y stress creates pure bending (marked as 'M', or 'pure M');
- uniformly distributed τ_{xy} stress creates pure torsion (marked as 'T', or 'pure T');
- sinusoidally distributed τ_{xy} stress creates pure shear force (marked as 'V', or 'pure V');

Note, the internal stresses are defined without performing a formal linear static analysis, i.e., similarly to the finite strip method, see Cheung and Tham (1997), we assume the internal stresses and connect them directly to section-level actions, as opposed to common numerical stability analysis where loads are applied and these are used to find the internal stresses. Another remark is that the above loads/stresses can arbitrarily be combined.

2.4 Stiffness matrices, buckling analysis

By using the theorem of stationarity of the potential energy, we need to take the partial derivatives of the potential energy function with respect to the Fourier coefficients, which leads to a system of n linear equations. The equation system is homogeneous, and can be identified as a generalized eigen-value problem. It can be expressed as follows:

$$\mathbf{K}_e \boldsymbol{\Phi} - \lambda \mathbf{K}_g \boldsymbol{\Phi} = \mathbf{0} \quad (16)$$

where \mathbf{K}_e and \mathbf{K}_g are the elastic and geometric stiffness matrices. The \mathbf{K}_e matrix is derived from the displacement functions, while \mathbf{K}_g is dependent on the involved stresses. Dependency of the geometric stiffness matrix on the stresses is linear, therefore it can be expressed as $\lambda \mathbf{K}_g$ where λ is a load multiplier. Moreover, $\boldsymbol{\Phi}$ is the displacement vector containing the displacement degrees of freedom (which in this solution are the Fourier coefficients), and $\boldsymbol{\Lambda}$ is a diagonal matrix which contains the λ critical load multipliers.

When constructing the stiffness matrices, the effect of supports must be considered. Two approaches are implemented. In the first approach the supports are modelled by linear springs, which can be defined at arbitrary positions over the cylindrical surface. If this approach is followed, additional stiffness terms are added to the elastic stiffness matrix. (Note, unlike in classic FEM, even one single spring means added stiffness in all the elements of the elastic stiffness matrix due to the Fourier series.) The second approach applies constraint equations to ensure zero (or: arbitrary non-zero) displacement at a given, arbitrary location. The constraint equations reduce the problem size, i.e., the effective DOF number is reduced. Note, for the second approach when the constraint equations are introduced, the DOF solved for are no longer directly associated with the Fourier coefficients and a secondary step to transform back to the unconstrained DOF is required to process the results in a general form.

3. Sample results

The developed method is able to perform linear buckling analysis for a wide range of problems, for pure or combined loading, with virtually arbitrary supports, for an extremely wide range of tube geometries. The numerical experience is that the necessary number of Fourier terms is small, i.e., the resulting number of displacement degrees of freedom (DOFs) is much smaller compared to that required in a shell FEM analysis. However, what Fourier terms are “necessary”, is strongly dependent on the problem; namely, it is dependent on the load type, on the member length, on the support conditions, and on whether we want to focus on the first buckling mode only or want to have higher modes, too. In the following subsections sample results are shown. In all the examples standard steel properties are used: $E = 210$ GPa, $\nu = 0.3$.

3.1 Pure load cases, first buckling mode

To study the first buckling modes, we have considered a wide range of R/t ratios between 10 and 500, as well as an extremely wide length range. In Fig. 2 first-mode critical loads for various pure loads are plotted with respect to the Ω non-dimensional length parameter, defined as:

$$\Omega = L/R \sqrt{t/R} \quad (17)$$

In Figs. 3-6 sample buckling shapes are presented. (Note, according to Ding et al, 2022, practical wind turbine tower segments are characterized by R/t between 30 and 150; typical L/R ratio for a tower segment is between 5 and 20, while it is between 40 and 70 for a whole tower. Thus, e.g., practical tower segments have Ω non-dimensional length between 0.5 and 5.)

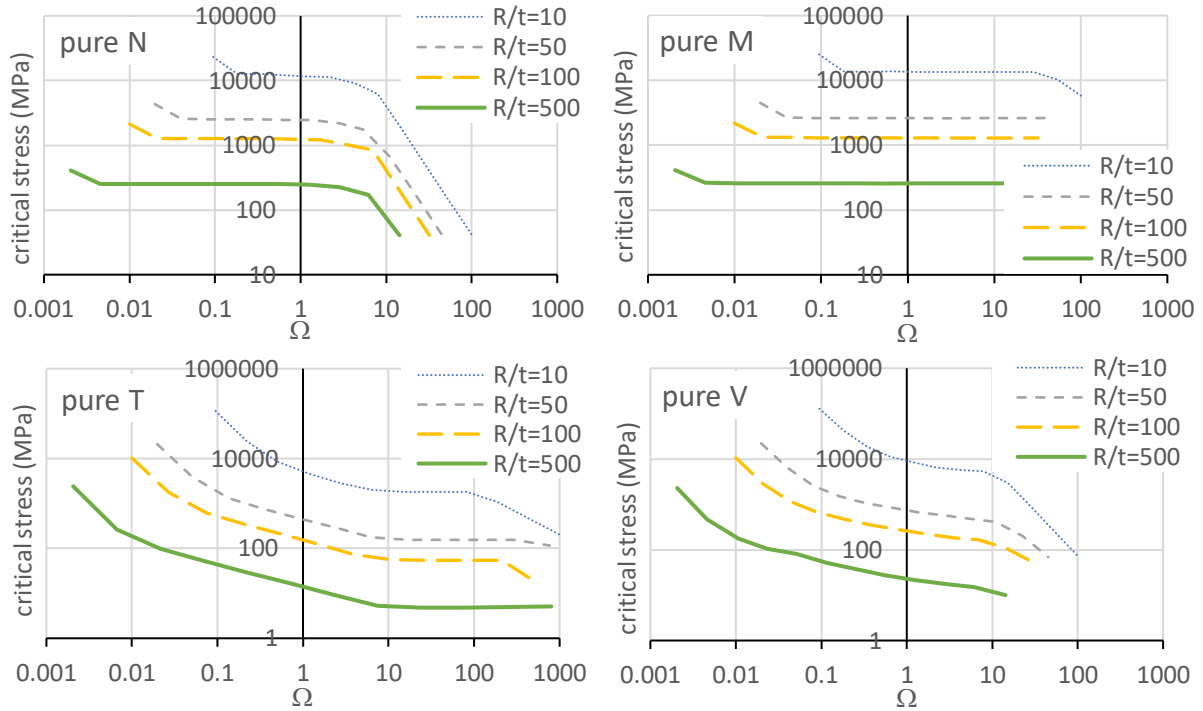


Figure 2: Critical stresses for pure loads

In the case of ‘pure N’, the well-known results are reproduced: if the member is very short, the barrel-type (axisymmetric) mode comes first, for large lengths the member buckles in the global (flexural) mode, while for a wide range of intermediate lengths we observe buckling with a varying number of circumferential and meridian lobes. The critical load results are slightly dependent on the end supports, but for classic hinged supports the critical load values from the method coincide with classic analytical solutions. The numerical experience is that it is enough to consider 5-6 Fourier terms in the longitudinal direction and 6-8 modes in the circumferential direction to get the first critical load with high precision.

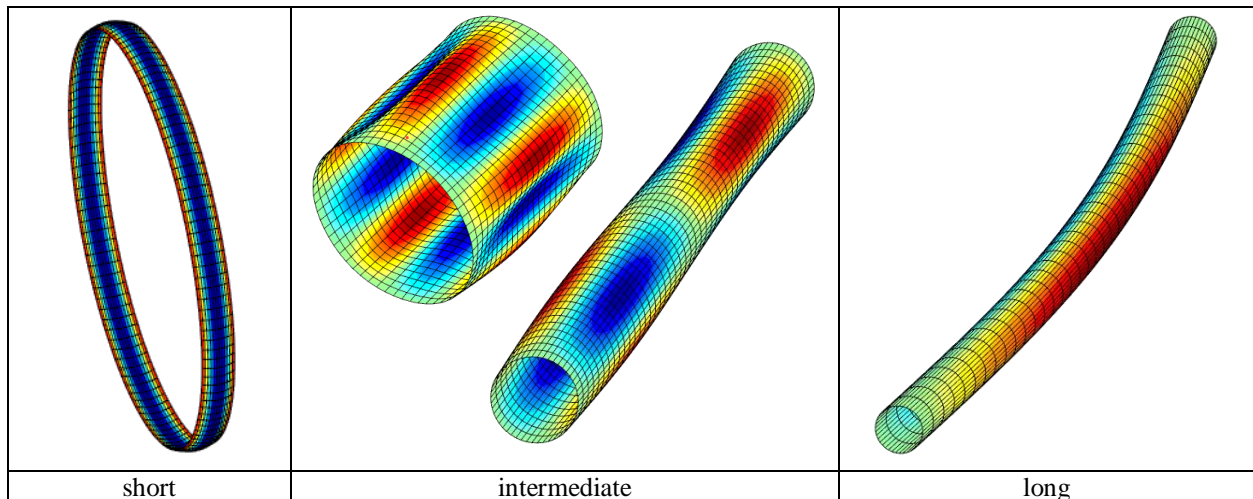


Figure 3: Sample buckling shapes: pure N, first modes

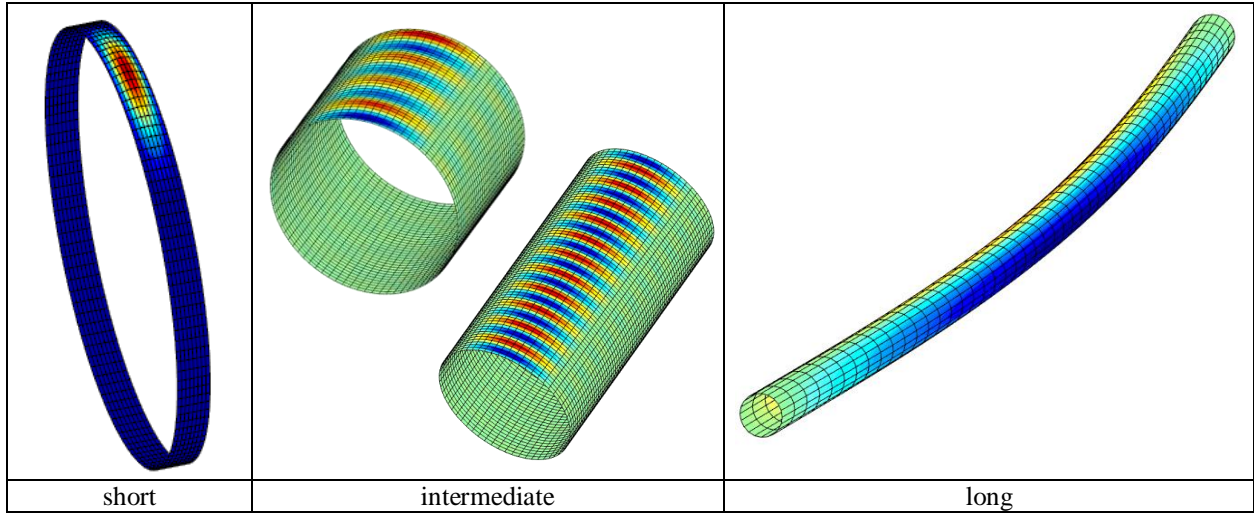


Figure 4: Sample buckling shapes: pure M, first modes

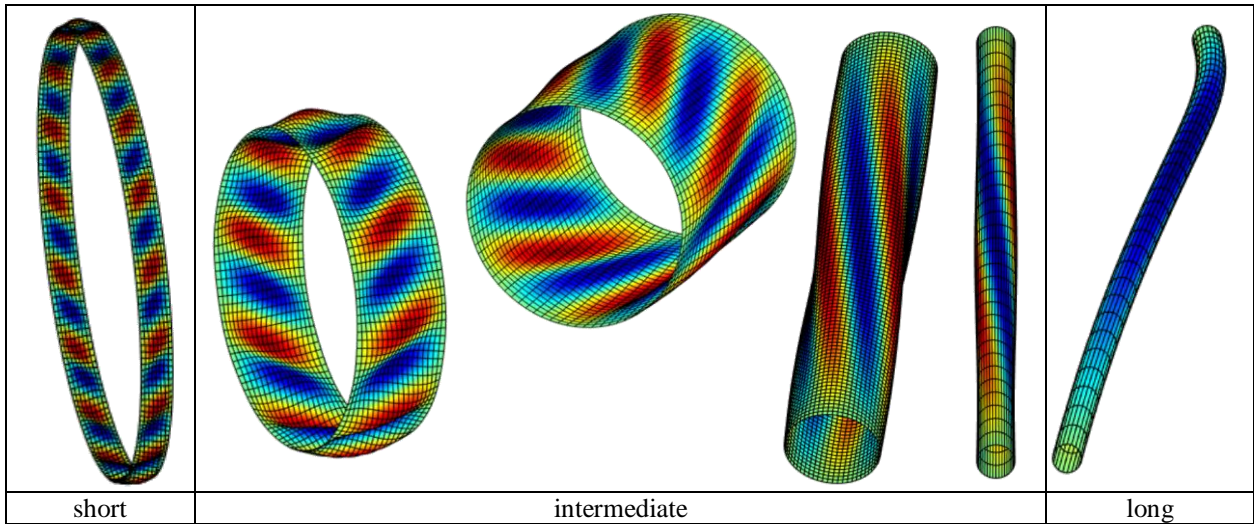


Figure 5: Sample buckling shapes: pure T, first modes

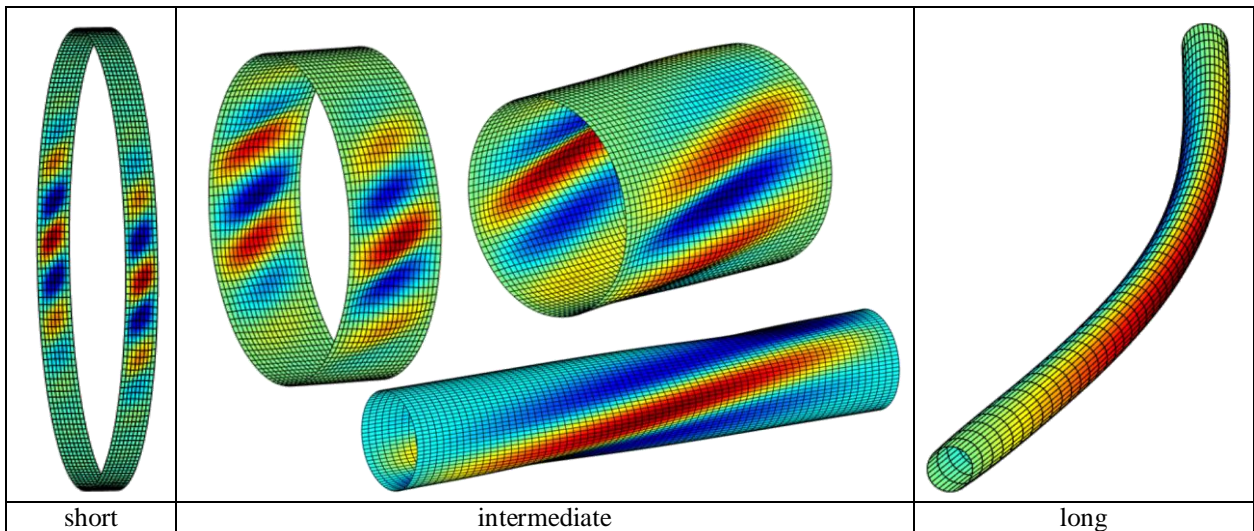


Figure 6: Sample buckling shapes: pure V, first modes

In the case of ‘pure M’, unless the member is extremely long, the first buckling mode is characterized by one single circumferential lobe: if the member is very short, there is one single meridian lobe, otherwise the number of meridian lobes is proportional with the member length (while the half-wavelength and critical load being nearly constant). Though it is rarely reported in the literature, a global mode does exist, which is a lateral-torsional buckling (but with extremely small twisting rotation). However, the global mode can be the first one only if the member is extremely long (e.g., if $R=100$ mm and $t=1$ mm, the member length should be more than 100 m!); that is why this mode has little practical relevance. For the necessary number of Fourier terms, the numerical experience is as follows. In the circumferential direction numerous terms are necessary: the shorter the member, the more terms are needed; 20-25 terms are practically enough even if the member is very short. In the longitudinal direction only a few terms are necessary, however, those terms which have half-wavelength approximately identical to the characteristic length of the buckling lobe are needed. For the local mode this length is a small one (and can well be predicted analytically), for global mode this length is a large one (in the vicinity of the member length).

In the case of ‘pure T’, the lowest buckling mode is characterized by one lobe in the longitudinal direction, while the number of circumferential lobes is inversely proportional to the member length. In the case of short members the inclination of the buckling lobes is approx. 45 degree, and as the member length increases, the lobes are less and less inclined (w.r.t. the longitudinal axis). At very large lengths the buckling is global, i.e., without cross-section distortion; the shape of the longitudinal system line is helical. The number of necessary Fourier terms in the circumferential direction is proportional to the number of circumferential lobes; this means that more and more terms are necessary as the member length decreases (without bound). Practically, 30-40 terms are sufficient for nearly any, even very short member. In the longitudinal direction: unless the member is long enough to have the helical mode, the number of necessary Fourier terms increases with the length. Numerically, the most demanding situation is, therefore, when the member is long, but not as long to experience helical buckling.

In the case of ‘pure V’ the behavior is essentially similar to that for ‘pure T’. Unless the member length is very large, there are multiple circumferential lobes; however, they are not uniform along the circumference. It is little known (if reported at all) that global buckling mode exists if the member is sufficiently long. This global mode is visually similar to a flexural buckling mode in the lateral direction (i.e., with translations perpendicularly to the shear force).

3.2 Combined load cases, first buckling mode

In this Section combined loading cases are demonstrated. In Fig. 7 interaction surfaces are presented for two tubular members. The surfaces represent the critical load factors, calculated by systematically varying the ratio of 3 selected loads (while keeping the fourth one equal to zero). The surface is generated by using normalized stresses, so that the load factor for the pure cases would be equal to one.

Sample buckled shapes are shown in Fig. 8. These buckled shapes are the first modes of a member with dimensions $R = 100$ mm, $t = 1$ mm, $L = 400$ mm, and with end cross-sections clamped. In the figure, e.g., $0.6N+0.4V$ should be interpreted as the stress in the member is combined from 0.6 times the critical stress to pure N and 0.4 times the critical stress to pure V.

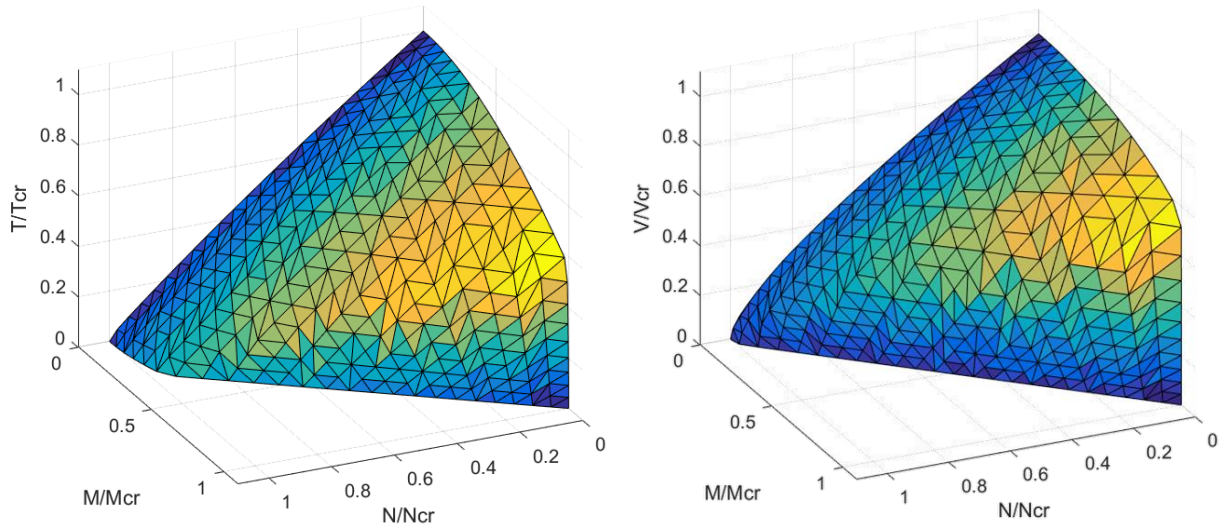


Figure 7: Interaction surfaces for LBA in the case of combined loading

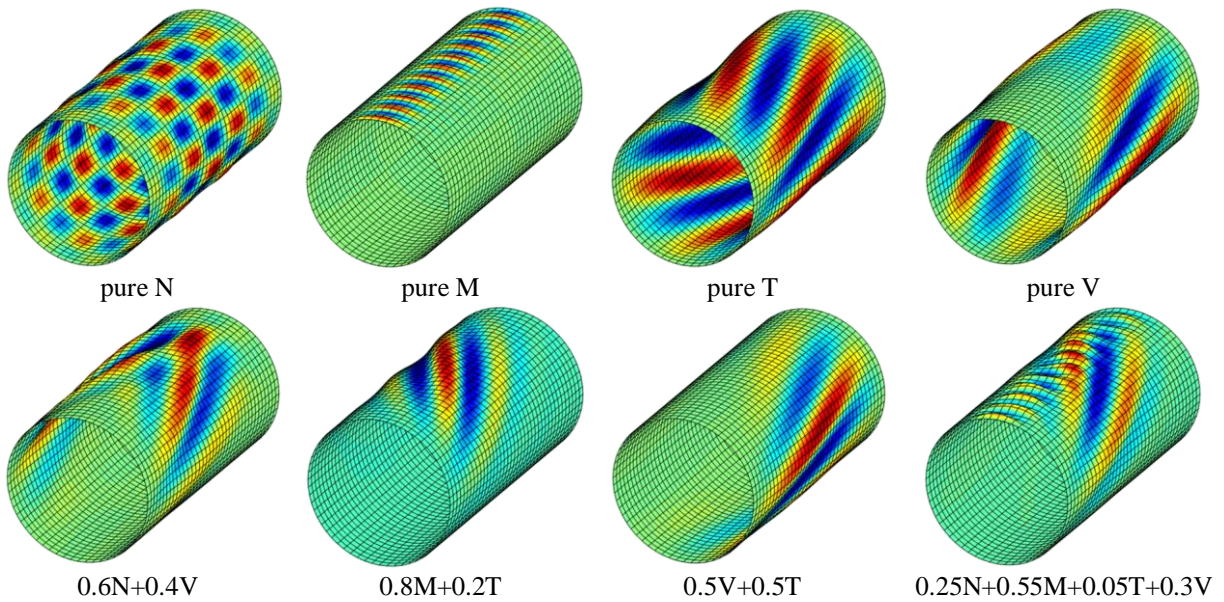


Figure 8: Sample first-mode buckling shapes for various load combinations

From the numerical studies it is observed that the handling of combined loading does not require any particular difficulty. The necessary number of Fourier terms can be determined from those of the pure cases (as discussed above), considering the member geometry and the loads from which the resultant loading is combined. Further, the interaction surface is nonlinear, thus the stability of a tube under combined loading is best considered under the actual loading state, as opposed to simple superposition of the pure load cases.

3.3 Pure load cases, higher buckling modes

Calculation of higher buckling modes is obviously possible. The only practical issue is that higher modes typically needs more Fourier terms to be calculated with high precision. The number of necessary Fourier terms is highly dependent also on how many modes are intended to be calculated.

As an example, Fig. 9 shows how the critical loads increase with mode number, in the case of various pure loads. The plots show the first 400 modes for a tubular member with $R = 100$ mm, $t = 1$ mm, $L = 800$ mm. As is well-known, in the case of pure compression there is a very large number of modes with nearly identical critical loads. In the case of other loads, the critical load values are increasing much more rapidly as higher and higher modes are considered.

It is also known that, if the member is in pure compression, and if the member is infinitely long, and if a particular shell theory is applied, the member has infinite number of modes with a critical load value equal to that of the first mode. If the associated longitudinal and circumferential buckling lengths (i.e., half-wavelengths) are plotted in a specific relative (non-dimensionalized) coordinate system, the solutions form a half-circle, known as Koiter-circle (Koiter, 1945). In practical cases (i.e., finite member length with some boundary conditions), there are finite number of modes, and the critical loads are not identical, still, the solutions can be plotted just as the Koiter-circle, and the solutions will scatter around a half-circle (Spagnoli, 2003). Such plot is shown in Fig. 10, created from the results plotted on Fig. 9 for ‘pure N’.

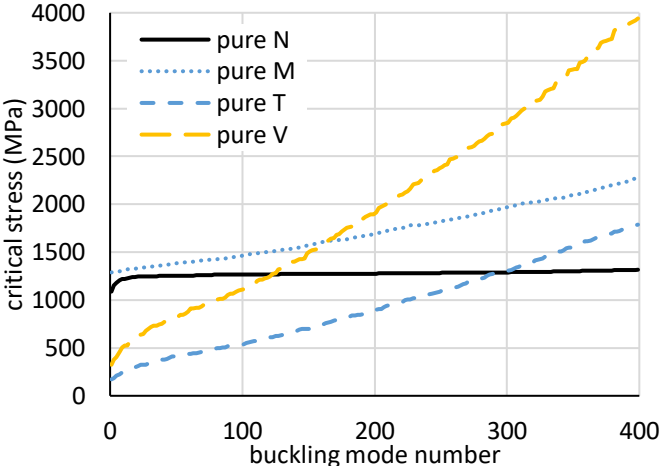


Figure 9: Critical stresses for higher buckling modes

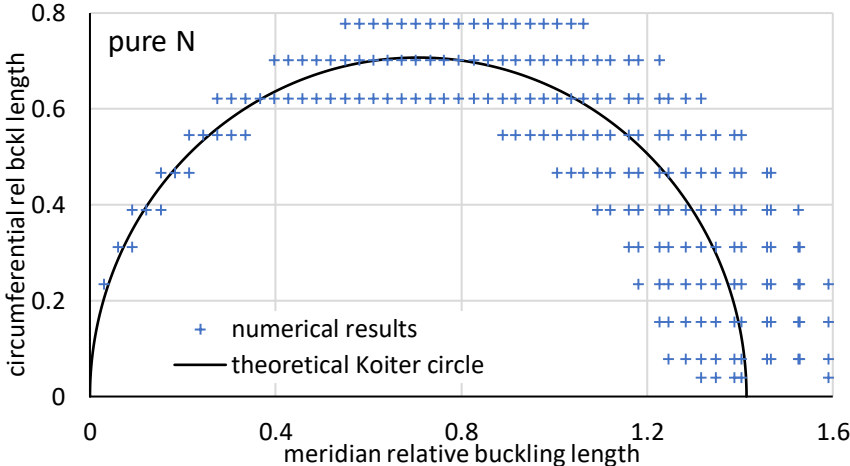


Figure 10: Representation of higher buckling modes by the Koiter-circle

4. Discussion

An advantage of the method developed herein is that it leads to an equation system much smaller compared to a shell finite element solution, while at the same time much more general than available analytical solutions. A potential further advantage of the method is that spectral analysis of the results can readily be performed since the solution is obtained in the form of Fourier series. This feature is already implemented, though not discussed in this paper. Moreover, the implemented spectral analysis can be utilized for any displacement field, e.g., for measured geometric imperfections of real tubular members. In fact, such work has already been initiated, and will be reported in future publications.

The method herein was also supplemented by a tool to determine the shape of the buckling lobes. From the shape, the characteristic buckling lengths in any direction can be calculated. The notion of ‘buckling length’ is classical, widely used in buckling analysis of columns, beams, and frames, but hardly applied to shell buckling. The developed tool makes it possible to discuss the shell buckling problem from the aspect of buckling length. Moreover, again, the same tool can and was extended to study other displacement fields, such as geometric imperfections of real tubular members; the results of which will be reported in future papers.

Finally, it is to mention that though the Fourier-series approximation does not require discretization, the here introduced method was extended so that the member can optionally be discretized longitudinally. The longitudinal discretization is numerically beneficial since the number of longitudinal Fourier terms within a segment can be reduced which makes the calculation faster and numerically more reliable. Moreover, it is known that practical wind turbine towers are globally (slightly) tapered and change in dimension “can” by “can” along their length, hence the longitudinal discretization enables the consideration of the cross-section changes, i.e., makes it possible to describe the geometry of practical wind turbine towers more exactly. Finally, the discretization makes it possible to consider non-uniform loading along the length, which again provides with the opportunity of having a more realistic model of practical wind turbine towers.

5. Conclusions

In this paper a newly developed numerical method was presented for stability analysis of tubular members under any combination of compression, bending, torsion, and shear with arbitrary end boundary conditions. The method uses full Fourier series to approximate the displacements of the tube. The advantage of the developed method is that it leads to an equation system much smaller compared to a shell finite element solution, while at the same time much more general than available analytical solutions. A series of examples illustrate the potential of the approach. Open source software, and various extensions to the method’s use for improving the efficiency of the design of wind turbine support towers, are underway.

Acknowledgments

This material is based upon work supported by the National Science Foundation under Grant No. 1912481 and No. 1912354. Any opinions, findings, and conclusions or recommendations expressed in this material are those of the authors and do not necessarily reflect the views of the National Science Foundation.

References

- Cheung, Y.K., Tham, L.G. (1997) "Finite Strip Method" CRC Press
- Ding, V., Abdelrahman, A.H.A., Lin, D., Shields, M.D., Myers, A.T., Krabbe, M., Schafer B.W. (2022). "Classical and Finite Element Methods for Elastic Buckling of Cylindrical Shells". Proceedings of the Annual Stability Conference, Structural Stability Research Council, Denver, Colorado, USA, March 22-25, 2022. p 20.
- Donnell, L. H. (1933). "Stability of Thin-Walled Tubes Under Torsion" National Advisory Committee for Aeronautics. Report No. 479.
- Flügge, W. (1962). "Stresses in Shells" Springer-Verlag, p 499.
- Koiter, W. T. (1945). "The Stability of Elastic Equilibrium" TU-Delt. English Translation by E. Riks, provided by U.S. Air Force Flight Dynamics Laboratory.
- Mahmoud, A., Torabian, S., Jay, A., Myers, A., Smith, E., Schafer, B.W. (2015) "Modeling protocols for elastic buckling and collapse analysis of spirally welded circular hollow thin-walled sections" Proceedings of the Annual Stability Conference, Structural Stability Research Council, Nashville, Tennessee, March 24-27, 2015. p 16.
- Sadowski, A.J. (2019). "On the advantages of hybrid beam-shell structural finite element models for the efficient analysis of metal wind turbine support towers" Finite Elements in Analysis and Design, Vol. 162. pp. 19-33. doi.org/10.1016/j.finel.2019.05.002.
- Sanders, J.L. (1963) "Non-linear theories for thin shells" Quarterly of Applied Mathematics, Vol 21(1), pp. 21–36.
- Silvestre. (2007). "Generalised beam theory to analyse the buckling behaviour of circular cylindrical shells and tubes" Thin-Walled Structures, 45, pp. 185-198.
- Spagnoli, A. (2003) "Koiter circles in the buckling of axially compressed conical shells", International Journal of Solids and Structures, Vol 40, pp. 6095–6109.
- Timoshenko, S.P., Gere, J. M. (1961). "Theory of Elastic Stability" McGraw Hill (reprinted by Dover in 2009), p 541.